International Journal of Earth, Energy and Environmental Sciences
ISSN: 2517-942X
Vol:14, No:7, 2020

Sediment Wave and Cyclic Steps as Mechanism for Sediment Transport in Submarine Canyons Thalweg

Taiwo Olusoji Lawrence, Peace Mawo Aaron

***Abstract*—**Seismic analysis of bedforms has proven to be one of the best ways to study deepwater sedimentary features. Canyons are known to be sediment transportation conduit. Sediment wave are large-scale depositional bedforms in various parts of the world's oceans formed predominantly by suspended load transport. These undulating objects usually have tens of meters to a few kilometers in wavelength and a height of several meters. Cyclic steps have long long-wave upstream-migrating bedforms confined by internal hydraulic jumps. They usually occur in regions with high gradients and slope breaks. Cyclic steps and migrating sediment waves are the most common bedform on the seafloor. Cyclic steps and related sediment wave bedforms are significant to the morpho-dynamic evolution of deep-water depositional systems architectural elements, especially those located along tectonically active margins with high gradients and slope breaks that can promote internal hydraulic jumps in turbidity currents. This report examined sedimentary activities and sediment transportation in submarine canyons and provided distinctive insight into factors that created a complex seabed canyon system in the Ceara Fortaleza basin Brazilian Equatorial Margin (BEM). The growing importance of cyclic steps made it imperative to understand the parameters leading to their formation, migration, and architecture as well as their controls on sediment transport in canyon thalweg. We extracted the parameters of the observed bedforms and evaluated the aspect ratio and asymmetricity. We developed a relationship between the hydraulic jump magnitude, depth of the hydraulic fall and the length of the cyclic step therein. It was understood that an increase in the height of the cyclic step increases the magnitude of the hydraulic jump and thereby increases the rate of deposition on the preceding stoss side. An increase in the length of the cyclic steps reduces the magnitude of the hydraulic jump and reduces the rate of deposition at the stoss side. Therefore, flat stoss side was noticed at most preceding cyclic step and sediment wave.

***Keywords*—**Ceara Fortaleza, sediment wave, cyclic steps, submarine canyons.

I. Introduction

SUBMARINE canyon are steep V-shaped walled (Shepard 1981) erosional feature, one of the most obvious deep-water seabed features on continental break down slope. They act as conduits for sediment transfer from the continental shelf/inter slope accommodation space to the deep-sea abyssal [1]-[4]. Canyons are common on continental slopes [5], shelve-incising canyons commonly develop across tectonically active continental margins and are most abundant along the western margins of both South America and North America [6], [7]. Submarine canyons evolve through geological time channelizing sediment gravity flows [8] that originated mostly from the continents due to tectonism and earthquake [8]. Canyons and gullies are an integral part of slope morphology on continental margins (e.g. [9]-[11]). Gullies are straight regularly spaced channel [12], formed by erosional processes 11], [13] or depositional processes [14]. The evolution of submarine canyon has been extensively discussed [15]-[18]. Submarine canyon origin and processes for transporting sediment is not fully understood [19]. 3D seismic interpretation remains the best method to analyze their evolution. Canyon architectural elements [20], [21] include large delta front valleys at the trough of a prograding seafloor slope settings; long fan valley that flow seawards to the abyssal. The capability of the canyons to act as sedimentary conduits depends largely on the rate of sediment supply at their heads [18] as well as the erosional processes at the canyon thalweg. Canyons are formed by erosive processes [22] that could as well give rise to bedforms such as sediment waves, antidunes and cyclic steps. This could influence the evolution and morphology of a canyon [23] such as working or reworking of the levee overbank. Canyons and gullies were seen to contain frames of crescent-shaped bedforms interpreted as cyclic steps [24], signifying the existence of sedimentary gravity flows in supercritical regime.

A bedforms are formed by interaction of a flow with the seafloor, including turbidity currents, thermohaline bottom currents, and tidal flow [25], [26]. The bottom of many continental shelves is covered with regular large-scale patterns of elongated bedforms with wavelengths ranging from several hundreds of meters to a few kilometers [27], [28]. Bedforms are common features in the submarine [29]. Understanding into the changing geometry, growth and migration of bedforms could give us an insight into the processes that initiate bedform architecture in Deepwater [30]. Bedforms derived from canyons deposit are present in much of the deep-water depositional settings [23], [31], [32], such as canyon-channel thalwegs, levee-overbanks, and channel-lobe-transition-zones [23], [31]-[34]. Most bedforms migrates upstream [35]-[38]. Several authors have studied sediment waves in different depo-belts such as continental slopes and rises e.g. [39], abyssal plains e.g. [40], deltas (e.g. [41]), canyons and channels (e.g. [42]) and volcanic flanks (e.g. [43]), continental shelves (e.g. [44], [45]). Sediment wave [35]-[37], is a submarine depositional feature that indicates channel lobe transition [38], [46], [47] where the channels are no longer confined by their levees. Sediment waves bedform are typically tens of meters to few kilometers in wavelength and few meters in wavelength height [35], [45]. The larger ones commonly appear in seismic profiles as gently

Taiwo Olusoji Lawrence is with the University of Aberdeen Geology and Petroleum Geology Department, AB24 3UE Aberdeen Scotland United Kingdom (corresponding author, phone: +44755-212-4871; e-mail: taiwosoji@gmail.com).

Peace Mawo Aaron, Department of Earth Sciences, Durham University, Science Labs, Durham DH1 3LE, UK (e-mail: peaceaaron@yahoo.com).

undulating, slightly climbing bedforms [48]. Most sediment waves originated from turbidity current [32], and are classified as bottom current sediment waves or turbidity current sediment waves. Bedforms migrate by eroding the upstream (stoss) side and deposition of fine-grained sediment on the downstream lee side through eddy current (interaction between water and the seabed classified bedforms based on their origin, migration direction, grain size and crest shape. Series of slowly collapsing and upstream migrating bedforms are referred to as cyclic steps [48]. Partially periodic wave-like bedforms [49] have wide range of asymmetry [48] (Fig. 1). The lee side abruptly drops steeply passing through a hydraulic jump before re-accelerating on flat stoss side, the flows are supercritical at the lee sides and subcritical at the stoss sides of the bedforms [50], [51]. Cyclic steps could also result due to turbidity current initiated by slope instability [52]. Upslope and downslope asymmetry are a characteristics of low and high energy settings, respectively, for both sediment waves and cyclic steps [48].

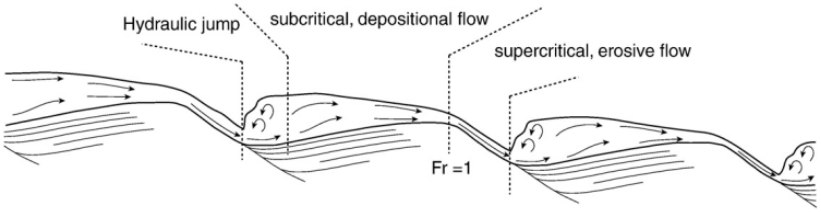

Fig. 1 Schematic drawing of a train of downslope asymmetrical cyclic steps (flow from left to right), beneath a turbidity current. It was assumed that turbidity current is accelerating from subcritical from the left border of the drawing, reaching the critical Froude number (Fr=1) at the crest before its further acceleration down the lee side of the bedform. The hydraulic jump is situated in the trough at the toe of the lee side. On the stoss side, flow depths are high and velocities low causing deposition and back-set bedding. On the lee side, the lower flow depth and higher flow velocities lead to erosion or limited deposition. Imbalance between the lee and stoss sides triggers upstream migration combined with possible aggradation. Modified from [23], [48]

Direct methods [45], [53], experimental methods [50], [51], [54] and numerical models [50], [55], [56], currently used for bedforms observation are not only inadequate but cannot be applicable to deep water bedforms analysis. Such observations will only reveal results that are based on analysis of deposits that has residual stratigraphic/geological records. There is an absence of unanimity on terminology and how deepwater bedforms should be interpreted [26], [45]. Seismic analysis of sediment wave has only been presented by few authors e.g. leveed channel systems in the Makassar Strait [57], deep-water Niger delta [57], Orinoco sediment wave field [58]. Seismic interpretation of bedforms has proven to be one of the best methods to understand how bedforms are formed and has enhanced the understanding of how it could be interpreted.

In this paper, we review the geomorphological evolution of bedforms as a mechanism for sediment transport in a submarine canyon thalweg and the relationship between the observed erosional features (e.g. gullies) and depositional features (e.g. waveforms) on the seabed. Here, we present a new 3D seismic dataset of the Ceara basin to study salient detailed sedimentary activities across the study area that are only recognizable in a very high-resolution bathymetric map. The improved high-resolution multi-beam echo sounders and 3D seismic data enables imaging the seafloor's complex nature to be unraveled (e.g. [17], [59]-[61]), this has further expanded the understanding of submarine slope features. We provide distinctive insight into the external factors that encourage bedforms transition and sediment transfer that could influence the evolution of Ceara Fortaleza basin. We reconstruct paleo-topographic features through a detailed mapping of seismic horizons/features. Sediment waveform was exported from the seismic volume of the study area (petrel platform) to global mapper where the cross-sectional parameters of the sediment wave (such as stoss side and the lee side) were extracted.

II. Geological Setting

Ceara Fortaleza Basin (Figs. 2 D & E) covers an area of 65,000 km^2 [62] offshore the city of Fortaleza (80 km north (pgs) (Brazil), with a water depth of 400 m [63] in the northeastern BEM (Fig. 2 D) [64]. The equatorial Africa and South America separation occurred during early cretaceous times [63], [65]-[68], and the Equatorial Atlantic opening occurred during Aptian-Albian [17], [69]. The post-breakup tectono-sedimentary evolution has been interpreted as behaving like an abnormal rifted margin such as the East Brazilian coast, with the main subsidence mechanisms driven by thermal and isostatic subsidence [63]. The separation of the Pangaea Supercontinent resulted in the formation of the Brazilian Cretaceous Rift System, forming passive continental margins and the Brazilian marginal basins (Fig. 2 A) [17], [70]. The Basin has three stages of evolution: rift (Neocamian-Eo-Aptian), post-rift (Neoaptian-Eo-Albian), and continental drift (Albian-Holocene) stages (Fig. 2 B) [71]. The rift, post-rift, and continental drift stages are characterized by continental, transitional, and marine megasequence deposits, respectively [17], evolution of the tectonic regime varies from predominantly normal (distension) to predominantly strike-slip (transtension and transpression) regime [63].

III. Dataset And Methodology

The dataset used for this interpretation is released by PGS, acquired at a water depth of 2000 m – 3000 m. The data

consist of high-quality 3D standard geometry seismic volume with bin dimensions (acquisition): 6.25 x 25 m, bin dimensions (processing): 12.5 x 25 m. The seismic lines were acquired with eight streamers each of length 6000 m with a separation distance of 100 m shot at 25 m intervals and 9000 ms record length. The dataset was processed via a fully ray-traced Kirchhoff Pre-Stack Time Migration (PSTM), Radon and residual. The dominant frequency of the dataset is 30 Hz, considering an average sediment interval velocity of 2000 m/s, the vertical 0 shows that the seismic volume is of high resolution.

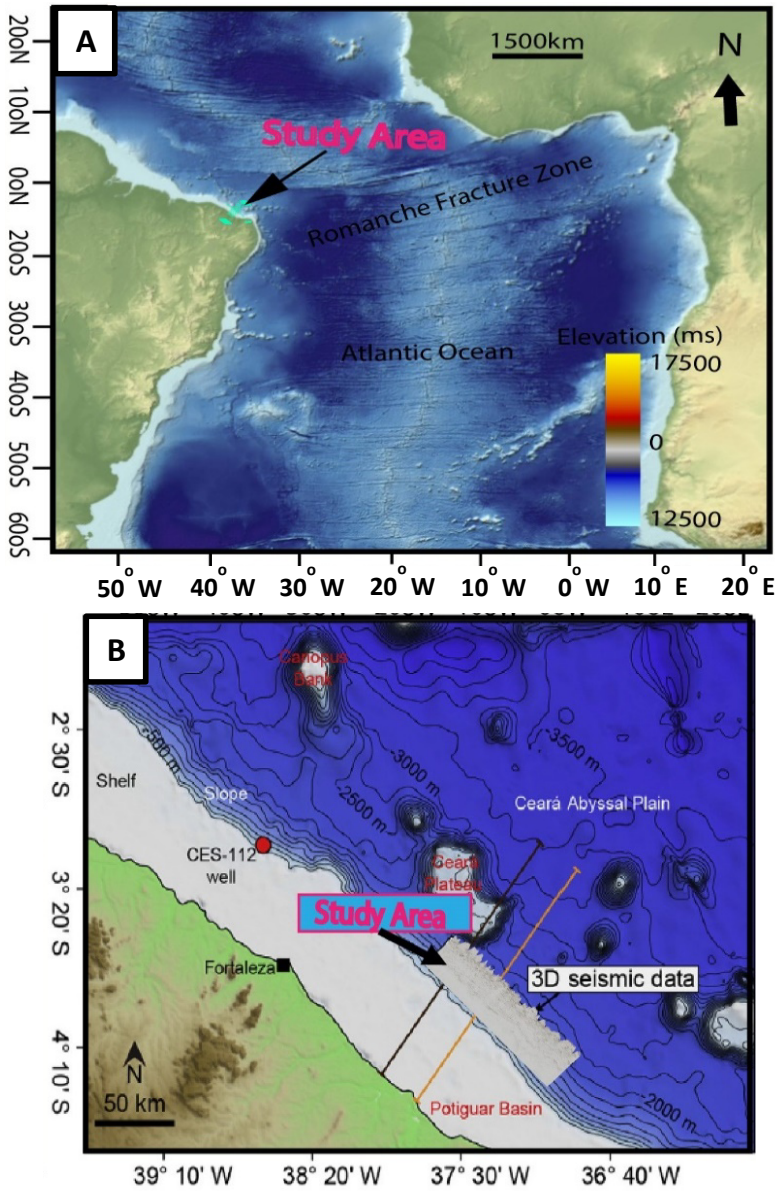

Fig. 2 A) Digital elevation model of the Equatorial Atlantic margin (edited from Petrel software) showing the BEM, B) Ceara Fortaleza Basin offshore the city of Fortaleza showing the study area 3D seismic section edited from [72]

As main methodology, we used the seismic interpretation/ regional mapping of the major horizons/stratigraphic intervals done through the Petrel platform. Major seismic horizons were identified and mapped, and the horizon surface map was created. RMS amplitude map and spectral decomposition was created, and reconnaissance of the dataset was done to know the potential presence and extension of the channel-lobe system. To reveal the thalweg debris mass flow, attribute computation/frequency decomposition – extracting and the range of frequency from the spectrum (taking the boundaries of the lobe) was done. To show the structural and stratigraphic edges of the lobe, the dominant frequency range and structural

decomposition based on edge detection approach (RGB blending) was done, and we delineate it and define the level of compartmentalization (Though we had a challenge to interpret the seismic sequence that define the compartment). The internal architecture of the identified bodies such as the lobe, channel and debris flow, was recognized in the seismic section as disrupted or chaotic low amplitude seismic facies underplayed by basal share surface of continuous reflection representing the failed mass.

The sediment waveform was exported from petrel platform to global mapper software where large bedforms and cyclic steps were evaluated and the parameters of each bedform were extracted. For each bedform, parameters were taken along a profile over the crest of the bedform; the stoss and lee slope length/angles, regional slope (slope of the entire bedform), degree of asymmetry (stoss length divided by lee length), wavelength and height were measured according to [73].

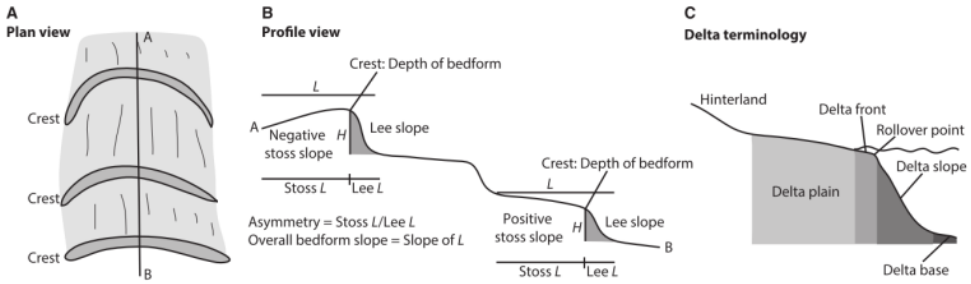

Fig. 3 Terminology and morphological properties calculated on bedforms observed on the delta slopes. (A) Plan view illustrating where the profiles were taken along the bedforms. (B) Profile view illustrating the different properties measured along the bedforms. (C) Delta terminology used in this study edited from [73]

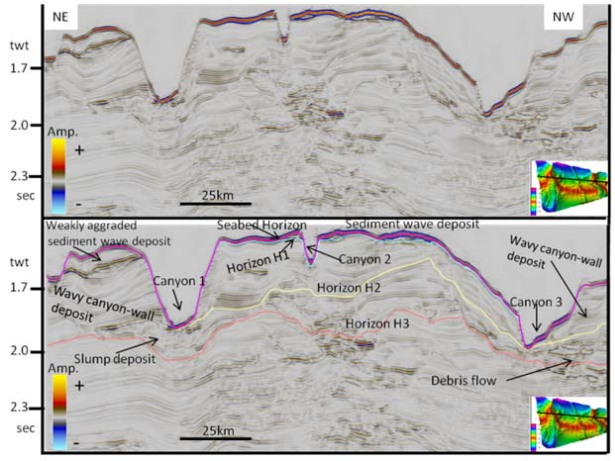

Fig. 4 Uninterpreted and Interpreted seismic section of Inline 1576 crossing the sediment wave region

IV. Result

A. Seabed Architectural Elements

The seismic section of the study area (Fig. 4) and seabed morphology surface map (Fig. 5 A) allow us to identify three canyons that incised the continental slope. Two active modern channels incised the seabed between canyon 1 and canyon 2, these brought about two different portions of sediment wave lobe deposit. The canyons are parallel to each other, they have low sinuosity, their width and depth vary with the water depth, the width of the canyons increase with an increase in water depth and the depth of the canyon incision increases towards the continent. The canyons have U-shape morphology characterized by several forms of bedforms at the thalweg, ranging from crescentic bedforms, cyclic steps and sediment wave. Most of the bedforms in the study area are tilting towards the north-west of the study area, this flow parameters are an obvious characteristic that could give us a hint that the flow direction of the canyons is from southeast to north west.

Undulated seabed bedform, similar to the ones described as Barerchan dunes [74], was observed on the seabed. The observed undulated furrows-like features (Fig. 5 A) have been completely draped at the distal area by a paleo-sediment wave but the furrows are still visible at the proximal part of the study area. The drape was incised by the two slim active channels (Figs. 5 A-C). The seismic section (Fig. 4) shows that the wall of canyon 1 has a wavy-like morphology, and a slump like bright transparent and chaotic seismic character at the lower left side wall, believed to have resulted from weak failure of sediment wave deposit. Canyon 1 has an average depth of 350 m and width of 1.8 km at the proximal end and narrows to 1.2 km and the distal part. Canyon 2 is believed to be more recent among the canyons and has the lowest sinuosity. Canyon 2 has the highest bright RMS amplitude reflection in the area, including its thalweg and overbank. The overbank shows cyclic steps and over spilling into the flank of canyon 1 with some evidence of canyon 1 wall collapse. Canyon 2 has semicircular crescentic bedforms and cyclic steps at its thalweg. The high amplitude chaotic reflection (Fig. 5 B) allows us to interpreted the crescentic bedform at the canyons thalweg to be composed of coarse grain sand sediment and the sediment waves are sandy occurring at latitude: 3° 43’ 2.6 and longitude: 37° 34’ 55.5. Two or more ends of the crescentic bedforms crest are pointing downslope and migrating downslope away from the flow source. The high amplitude reflection at the distal end of the two sides of the canyon wall could indicate that the sandy lobe was cut through by a high incision channel flow and divided the lobe into two parts, and has displaced some of the sand deposit

from the paleo sandy sediment wave to the two sides of the channel. Canyon 2 is the smallest canyon with an average with of 0.8 km and depth of 150 m. The space between canyon 2 and canyon 3 is characterized with various sizes of mounds and furrow like undulations, it is at the northwestern end of the study area, it has the largest canyon width of 3.5 km and an average depth of 500 m.

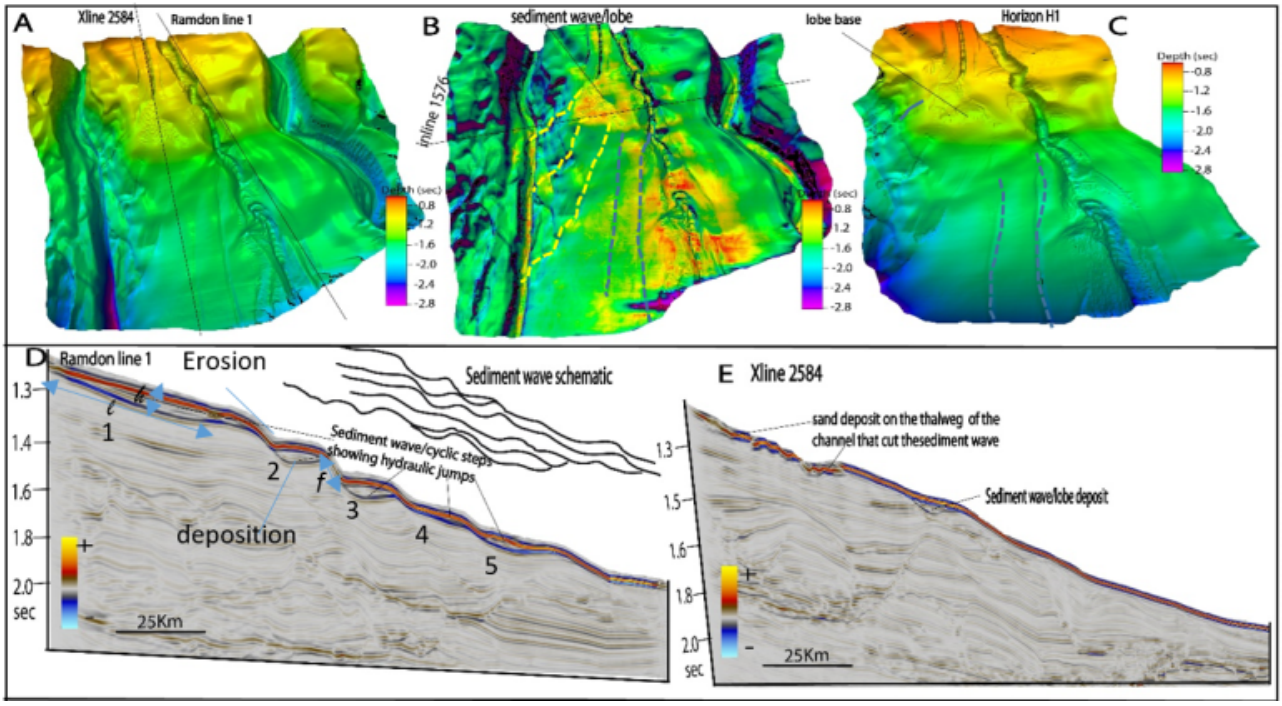

Fig. 5 (A) Seabed surface map showing Canyon 1, 2 & 3 (B) RMS Amplitude map of the Seabed showing high amplitude RMS sandy reflections at the canyons thalweg, hydraulic jumps and cyclic steps (C) surface map of horizon H1 below the seabed indication the base of the sediment wave lobe. (D) Seismic section of random line 1 showing symmetric sediment wave cyclic steps and hydraulic jump (E) Seismic section of Xline 2585 showing the sediment wave deposit at the channel thalweg

The seismic section (Figs. 5 D & E) gives us an insight into sediment wave interaction with canyons deposits. Patches of high amplitude reflection seen at canyon 3 thalweg (on the RMS surface map Fig. 5 B) could be due to sandy sediment swept from a canyon 2 levee and overbank. The elevated wall of canyon 3 could be responsible for shielding more of the sand sediment from migrating into the north western region serving as a sediment trap.

To critically analyze the observed bedforms in the study area, we grouped the bedforms into three sets (set A, set B, set C). Set A is the sediment wave bedform at the mouth of the recent active channel S2 (Fig. 6 set A, Figs. 5 A-C), set B is the crescentic bedforms and sediment wave on channel canyon 2 thalweg (Fig. 6 set B), set C is the lager bedforms including cyclic step and furrows (Fig. 6 set C). The height of the sediment wave in Set A is between the range of 32 m and 1.33 m and the maximum asymmetricity ration is 140, the sediment wave lobe of set A has an average slope of -3.58°. The height of Set B sediment wave is between the ranges of 54.23 m and 4.5 m with an average slope of -5.14°. Set C has a height range between 194 m and 9.5 m and an average slope of -4.78°. The combined graphical analysis of the sediment wave parameters is summarized in Fig. 7.

V. Discussion and Conclusion

A. Bedforms in Submarine Canyons

The origin of bedforms in submarine canyons has been debated [81], and many studies now suggest that they are formed by supercritical density flows (Froude number > 1) and cyclic steps [32], [33], [76], [86]. Bedforms observed in this study share analogous morphological characteristics as those studied in similar depobelts, where terms such as furrows, undulations, erosional scours, antidunes, dunes, sand waves, sediment waves, crescent-shaped bedforms, and cyclic steps were investigated [18], [33], [36], [38], [75]-[79]. The presence of elongated scours and scars on the seabed canyon flanks (Figs. 4 and 5) could suggest that continental break (deltafront) failure is responsible in initiating sediment density flows. The deeper canyons (Fig. 4) must have been eroded into the continental shelf during relative sea-level falls, which carries sediment from the shelf to the slope and into lower basin. The abrupt reduction of the canyon walls could be connected to failure of steep canyon walls which thereafter lead to mass movement with the evidence of slump and debris flow (Figs. 4 and 5). Coarse-grained deposits such as spillover lobes L1 & L2 (Figs. 5 B and 6 set C1) and crevasse splays have been observed on outer bend levees e.g. [80].

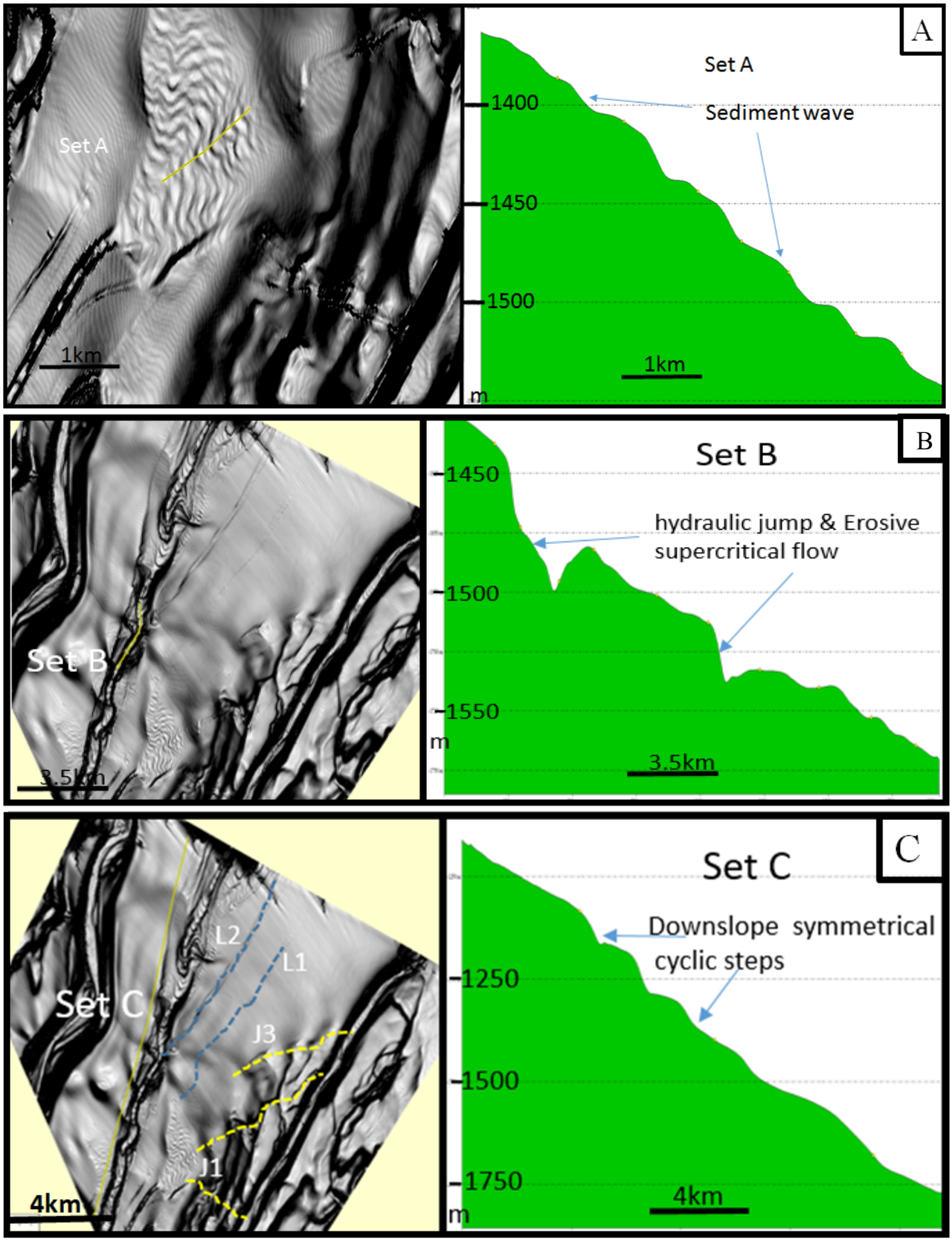
A
Set A
Sediment wave
1400
1450
1500
1km
m
Set A
1km
B
Set B
hydraulic jump & Erosive supercritical flow
1450
1500
1550
m
3.5km
Set B
3.5km
C
Set C
Downslope symmetrical cyclic steps
1250
1500
1750
m
4km
Set C
L2
L1
J3
J1
4km

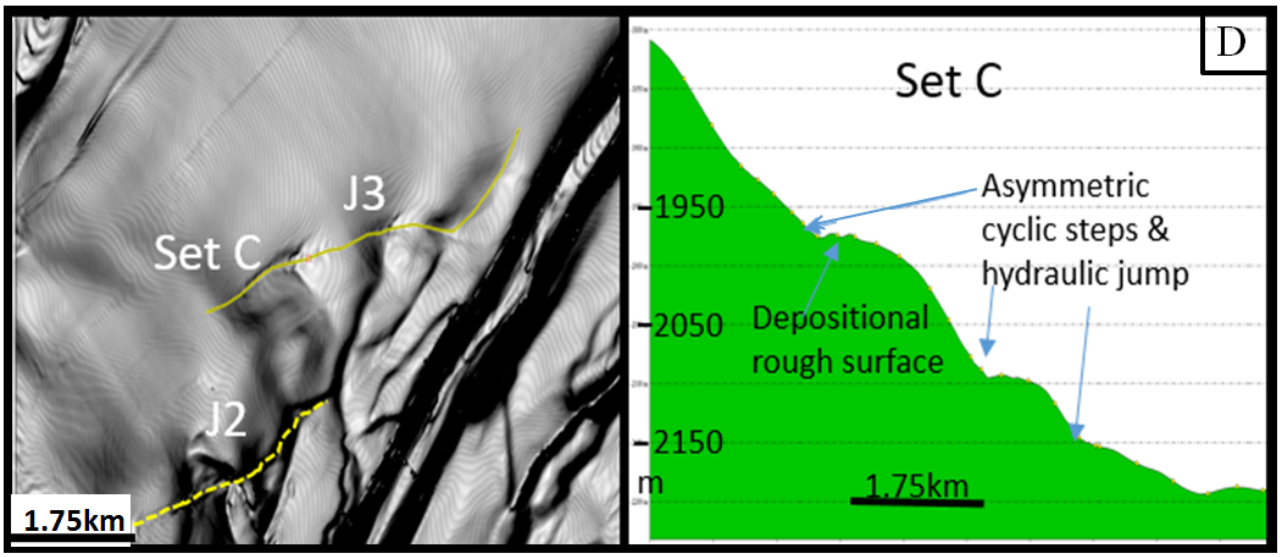

Fig. 6 Profile of sediment wave region: (A) set A, (B) Set B, (C) set C without hydraulic jumps, (D) Set C with hydraulic jumps

The crescentic bedforms observed in this study are often similar to bedforms observed in many submarine canyon and channel environments (Figs. 5 B, 6 B) [41], [73], [76], [81], [82]. Slope angle controls the gravitational driving force for sediment density flow; thus, the likelihood of a density flow becoming supercritical typically depends on slope angle [83]; density flows have been qualified as supercritical if the slope settings that is steeper than 0.6° [84], 1.15° [3], greater than 4° [73]. Stratification, as observed in the region of cyclic steps between the depth of 1.3(twt) and 2.0 s(twt) (Figs. 5 D & 6 set C) could be as a result of a high energy density flow that gave rise to cyclic steps and hydraulic jump. Submarine buried channel distortions (Fig. 9) are responsible for the lack of internal stratification at the deeper segment (Figs. 8 and 9). Deposit is formed from a very dense and coarse-grained near-bed layer at the base of the gravity [33] or because of strongly decreased bed traction due to a hydraulic jump [85]. Subcritical density flow could occur when the stoss side is comparatively flat compared to the subsequent wave, so that the erosional steep lee side produces supercritical density flows, as explained in cyclic steps (3). Hitherto, it has been postulated that the gap between small and large sediment waves is related to flow stratification [83], which builds on an established relationship between supercritical flow discharge and cyclic step lengths [32], [33].

Upstream migrating bedforms have been regarded to as cyclic steps [33]. We assigned each downward steeply dropping lee side of the bedform to be hydraulic fall (*f*) (1). This is the flow passing through a hydraulic jump before re-accelerating on the flat stoss side. This dune-shaped feature migrates upflow by the lee-side erosion and the stoss-side deposition, created by high energy turbidity current flow from the continental break (Fig. 5 D Random line). At a depth range of 1.3 ms to 1.8 ms, five cyclic steps were identified numbered 1 to 5 (Fig. 5 D) with dimensions (length *l* x height *h* x hydraulic fall *f*) as listed in Table I. The second and third cyclic steps are averagely symmetrical. The hydraulic jump magnitude *m* (Fig. 1) (2) depends on the depth of the hydraulic fall. The depth of the hydraulic fall *f* is directly proportional to the length *l* of a cyclic step and inversely proportional to the height *h* (rate of deposition) as it is the energy of supercritical flow that controls the deposition at the stoss side that is:

$$f \alpha \frac{l}{h} \quad (1)$$

Using the magnitude *m* of the hydraulic jump (that controls sediment deposition at stoss side) as constant of proportionality; we have:

$$f = \frac{l}{h} m \quad (2)$$

So that:

$$m = \frac{fh}{l} \quad (3)$$

TABLE I
PARAMETERS OF CYCLIC STEP

Cyclic step	*L(m)*	*h(m)*	*F(m)*	*l/h(m)*	*m(m)*
1	2370	84	488	28.21429	17.2962
2	890	95	488	9.368421	52.08989
3	891	95	366	9.378947	39.02357
4	1167	47	285	24.82979	11.47815
5	1735	50	150	34.7	4.322767

An increase in the height of the cyclic step means increase in the magnitude of the hydraulic jump, and thereby increases the rate of deposition on the preceding stoss side. Conversely, an increase in the length of the cyclic steps reduces the magnitude of the hydraulic jump as well as the rate of deposition at the stoss side, therefore a flat stoss side could be noticed at the preceding cyclic step. Giving rise to a dense and coarse-grained near-bed layer at the base of the gravity current

[45], [83] or a strongly decreased bed traction due to a hydraulic jump [85]. Similar morphology could be recognized at deeper depth indicating that similar process occurred in the past. The disorderly draped pattern observed in buried channel CH-2 (Fig. 9) could be due to the buried undulated furrows that was subsequently draped by sediment wave. The paleo-draping process forced two different parallel buried channels (Fig. 9, CH-2) to converge at some point and was also forced to bifurcate as it travels down. Looking at the draping style on the seabed stoss deposition, seismic section Xline 2584 (Fig. 5 E) and the surface map H1 (Fig. 5 C) of the sediment wave base, we could infer that the draping style is thickening downward while the sediment wave is thickening upward. Hydraulic jumps are increasingly recognized as an important part of depositional and erosional processes on the continental margin (e.g., [4], [31]). Several periods of hydraulic jumps were identified in this dataset (Figs. 5 D, Fig. 6). Flows over the cyclic steps are supercritical towards the lee face and decelerates at the hydraulic jump in the trough, there exist a waxing to critical flow at the stoss side near the crest but quickly become supercritical flow at the lee side. This process gave rise to deposition rough surface on the stoss side due to slowing of the flow energy and offloading of sediment (Fig. 6 set C). Mud-dominated currents tend to deposit the bulk of their suspended load downstream of the hydraulic jump [87]. We correlated each set (A, B, C) by plotting the height of the sediment wave against the wavelength (Fig. 6) in line with the proposition of [24]. The degree of asymmetricity of a sediment wave was evaluated by likening it to cyclic step aspect ratio findings by [33]. He postulated that aspect ratio is controlled by lee and stoss slope. We plotted the lee side slope length to the slope length of the stoss side. Set A, B & C sediment wave (Fig. 6) have an average slope of -3.58, -5.14 & -4.94. There is a good correlation between the wave height and wavelength (Fig. 11 Set A, B & C). The R^2 values of sets A, B and C are approximately 0.17, 0.10, 0.2, respectively. We further combined the three sets of sediment wave (Fig. 6 Combined set A, B & C H:L), the correlations show that the height of the sediment wave increased and migrates downslope (e.g. [88]).

All the sediment waves have comparable morphologies and are considered as small-scale cyclic steps compared with those observed in the marine environment [24], [31], [86]. Some discrepancy in the points that does not fall in line with the line of best fit could be due to variations in flow properties, flow thickness and sediment grain size [45]. In the case of cyclic step, the slope of the lee side increase density flows that have influence on the cyclic step origin and the magnitude of the hydraulic jump. The degree of asymmetricity is plotted in Fig. 6 set A-asymmetricity, Set B-asymmetricity, Set C-asymmetricity. The points plotted on Fig. 7 show a close correlation and further justify the prominence of density flow in the area. The graph of set A is more of symmetrical. Sediment wave asymmetry is observed mostly on the lower slope areas, while set B is more of crescentic wave on the channel thalweg and Set C is made of large scale bedform like a cyclic step & larger sediment wave. Most of the stoss sides of set B and set C (Fig. 7) are thick and table like flat, have their stoss side length increases because density flows require longer distances to become critical on lower slopes [73]. The lee side/angle is steeper than the stoss side with R^2 values of 0.05 and 0.09 with linear equation of y = 0.208x + 78.688, y = 0.3958x + 498.49, respectively. The linear equations indicate that the wavelengths are longer. Generally, longer wavelength and subsequent higher asymmetry are observed at the lower slope towards the NE-NW end of the dataset; at this point, ocean current could be the most driving force.

It could be inferred that the rate of erosion of the lee side depends on the acceleration of the flow, which further depends on the slope of the lee side; this in turn increases bedform heights on the stoss side due to deposition of the eroded sediment when the flow decelerates into the subcritical zone.

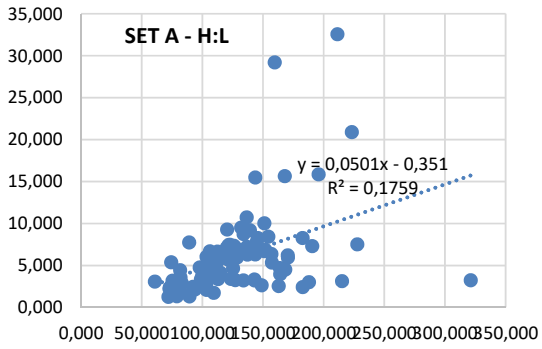

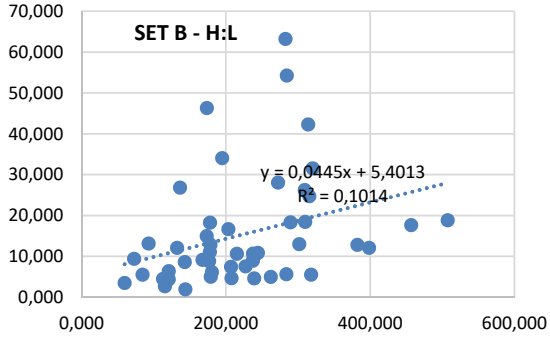

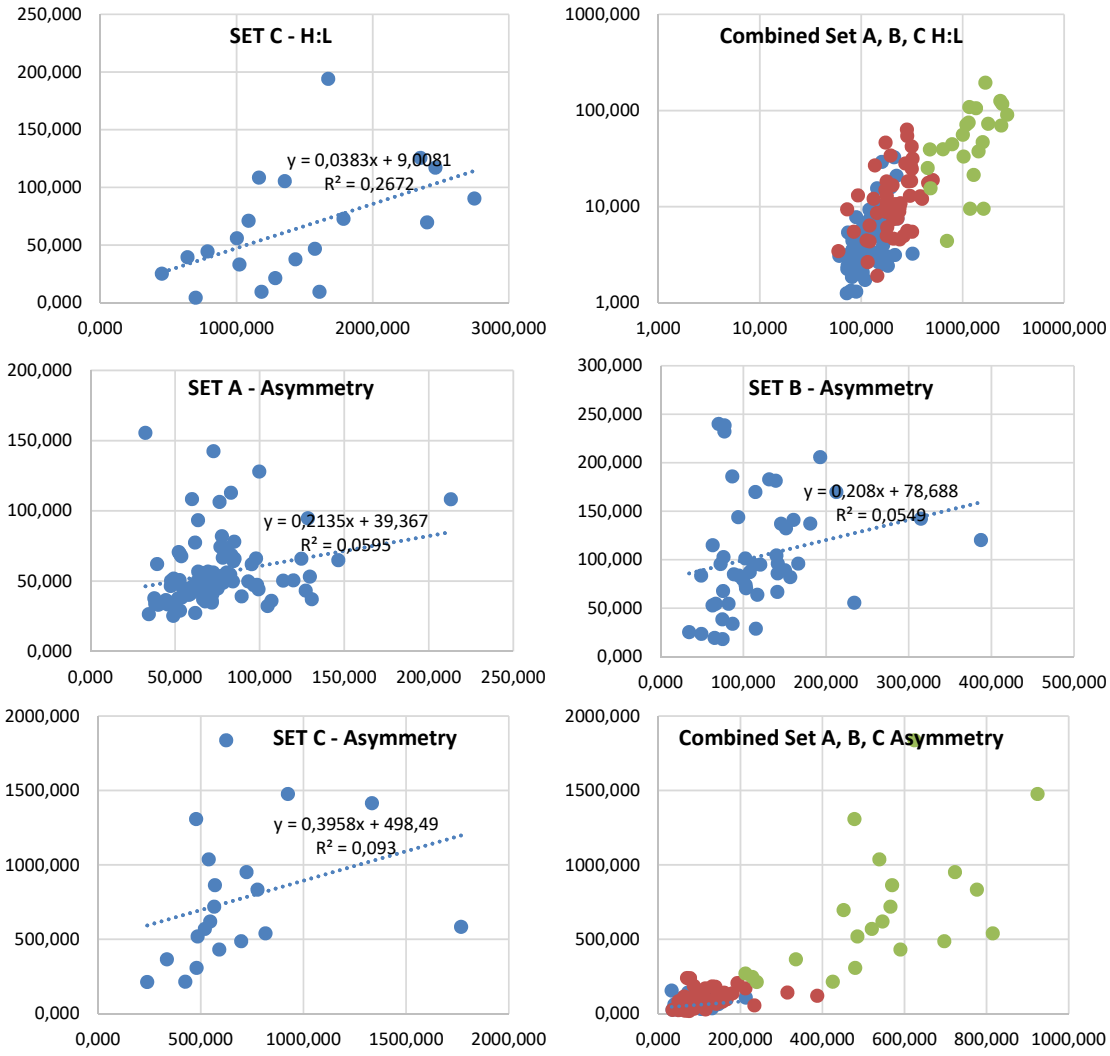

Fig. 7 Relationship between bedform morphological parameter

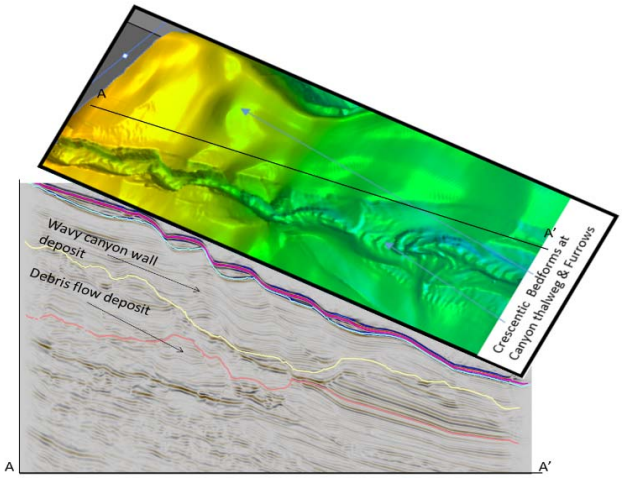

Fig. 8 Surface map and seismic section of seabed undulations showing how the morphology is transmitted to the deeper section

B. Bedforms and Debris Flow

Among the various geophysical techniques available for characterizing debris flows, 3D seismic attributes have proven to be some of the most useful tools [90]. The space between the boundary canyons are characterized by scour-undulated furrow-like features; this indicated that weak slope collapse has taken place in the past. The debris flow is defined by low-amplitude, parallel internal reflections that down lap onto underlying strata (Fig. 8). The initial sediment transport mechanism was debris flow seen from the transparent seismic reflection of the horizon mapped below the seabed (Figs. 5 C and 8). The seismic profiles show chaotic and disrupted strata and the accompanied slide surfaces within debris flow deposit and were separated from the much more continuous facies of non-MTD deposits such as described by [90]. The debris flow in the interval of interest (Fig. 9) lies on the remnants of older mass-transport deposits (MTDs) and buried channel system that might have been active at different times. Wedge ramps and flats indicate changes in the morphology of shear surfaces

in deeper MTDs, which relate to local stress fields and directions of transport during mass-wasting events [91]. Mass movement in the area is commonly debris flow and mudflow complemented by bedforms at the later stage, though from the medial parts most of the flow became relatively high energy fluidized similar to [92], this could be attributed to the lack of levee growth because the energy of the flow could not allow significant over bank deposit to aggrade.

C. Sediment Transfer

The use of Petrel perturbation impulse response brings to the surface sediment response to external changes, it indicates reaction of the dynamic sedimentary geologic processes relating to changes in the nature of sediments and the deviation of sediment movement/deposit in the basin over time from its normal state. Impulses can be characterized with different stratigraphic layers [89] or paths, caused by an outside influence most likely gravity. We considered the sediment wave region to model the architecture of sediment transfer architecture (Fig. 10) of the study area. We considered picked horizon surfaces at the sediment wave region only, namely: Seabed (seabed) horizon and Horizon H1 (lobe base) at a depth of circa 2.7s (twt). We use the petrel software impulse response tools to model sediment dynamic reaction with respect to burial depth. The bright red reflection (Fig. 10) represents a sandy sediment migration path. Sediment impulse response at H3 (the deepest horizon) is muddled most likely due to erosive events or unconsolidated sediment movement. The bright red reflections are seen to be moving from NE to NW but not as organized as the stratigraphic layer above it. Horizon H2 has more organized impulse reflection, the chaotic nature could be due to the channel's incisions at that layer. The response on the seabed indicates the present-day sediment movement from the NE to the NW of the study area, this could further support the reason why we have lighter seismic amplitude reflection at the northwestern part of the study are and gradually increase towards the northwest.

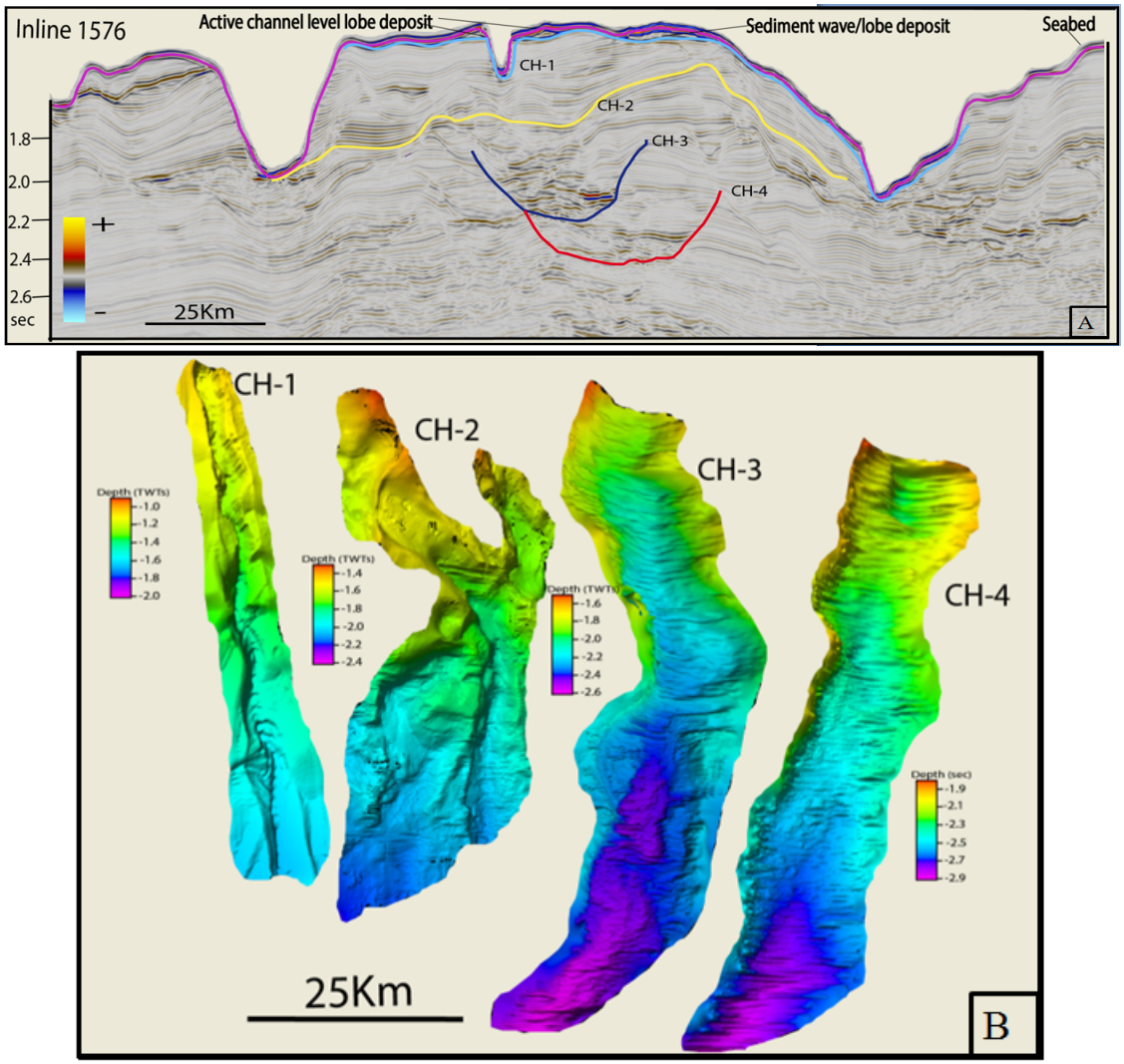

Fig. 9 Seismic section of BB' across sediment wave region, showing the interpretation of buried channels

The four low sinuosity buried channels (CH-1, CH-2, CH-3, CH-4 Fig. 11) observed were arranged in an alternating manner like a lobe like tributaries with the thalweg composed of high amplitude (coarse grained sand sediment) reflection. The high amplitude seismic reflection at the channels thalweg could give us a clue and further support the argument that the region was composed of buried sand sediment most likely from the paleo-sediment wave and it has been known that sediment wave deposits are sandy. The undulated ripples like feature within the channels indicated that a bottom currents sediment wave contributed in transporting sediment.

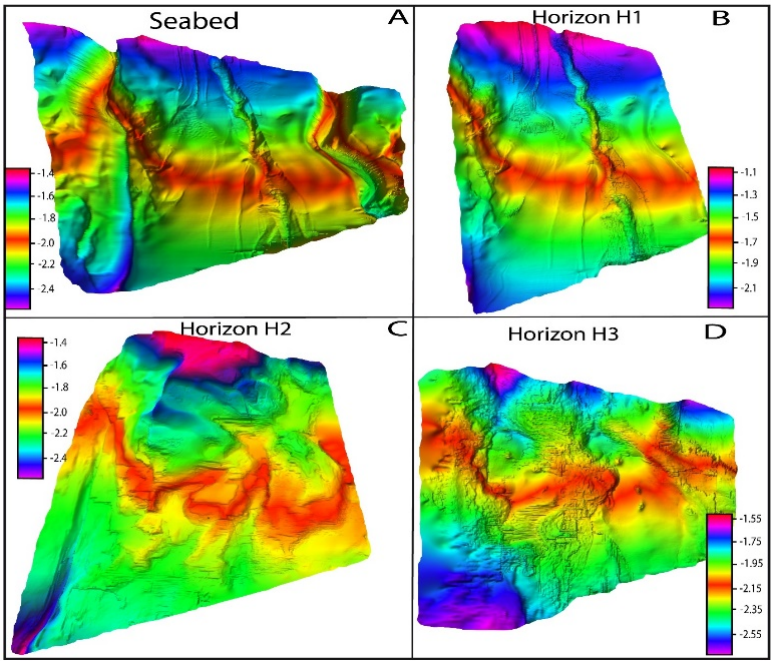

Fig. 10 Petrel perturbation impulse response of: (A) Seabed, (B) Horizon H1, (C) Horizon H2, (D) Horizon H3 showing sediment transfer impulse response from NE to NW

Assigning volume attributes such as acoustic impedance properties to the sand filled channels and surrounding and interbedded mud and clay layers could give us the general morphology of buried channel architecture [93]. We applied four different volume attributes, namely: Relative Acoustic impedance, Variance volume attribute, Amplitude contrast volume attribute and Reflection intensity volume attribute (Fig. 11) The orientation of the buried channels was tending from north-east to north-west, which could invariably imply the sediment transport orientation.

VI. Conclusion

- Sediment transport in canyon thalweg occurs as slowly migrating downstream processes are maintained by bedforms pointing upstream.
- Sediment waves in the study area migrate upward at the initiation stage, as it aggrades to the critical point, it collapses downstream to support the actual sediment transportation downstream.
- High amplitude coarse-grained reflections at the canyon thalweg shows that the most sediment waves have morphology signifying up current transport as in antidunes, while just a few collapsing or leftover waves appear to migrate down-current in the manner of dunes. Wavelength is seemingly certainly correlated to low velocity. Sand-rich sediment waves show quite different wavelength-to-height relationships to those formed dominantly of gravel as recorded in some articles.
- Waves prograde by depositing on up-current sides, including deposition of thicker and more frequent sand bodies.
- Large sediment waves such as cyclic steps were interpreted as supercritical flow bedforms, [32], [33]. This study brings to bear that bedforms such as cyclic steps are common signals of hydraulic jumps in submarine canyon, channel, levee-overbank, and channel lobe transition (Fig. 5) [31]-[33].
- The hydraulic jump magnitude depends on the depth of the hydraulic fall. The depth of the hydraulic fall is directly proportional to the length of the cyclic step and inversely proportional to the height h (rate of deposition) at the stoss side.
- An increase in the height of the cyclic step means an increase in the magnitude of the hydraulic jump and thereby increases in the rate of deposition on the preceding stoss side. Conversely, an increase in the length of the cyclic steps reduces the magnitude of the hydraulic jump as well as the rate of deposition at the stoss side, therefore a flat stoss side could be noticed at the

preceding cyclic step.

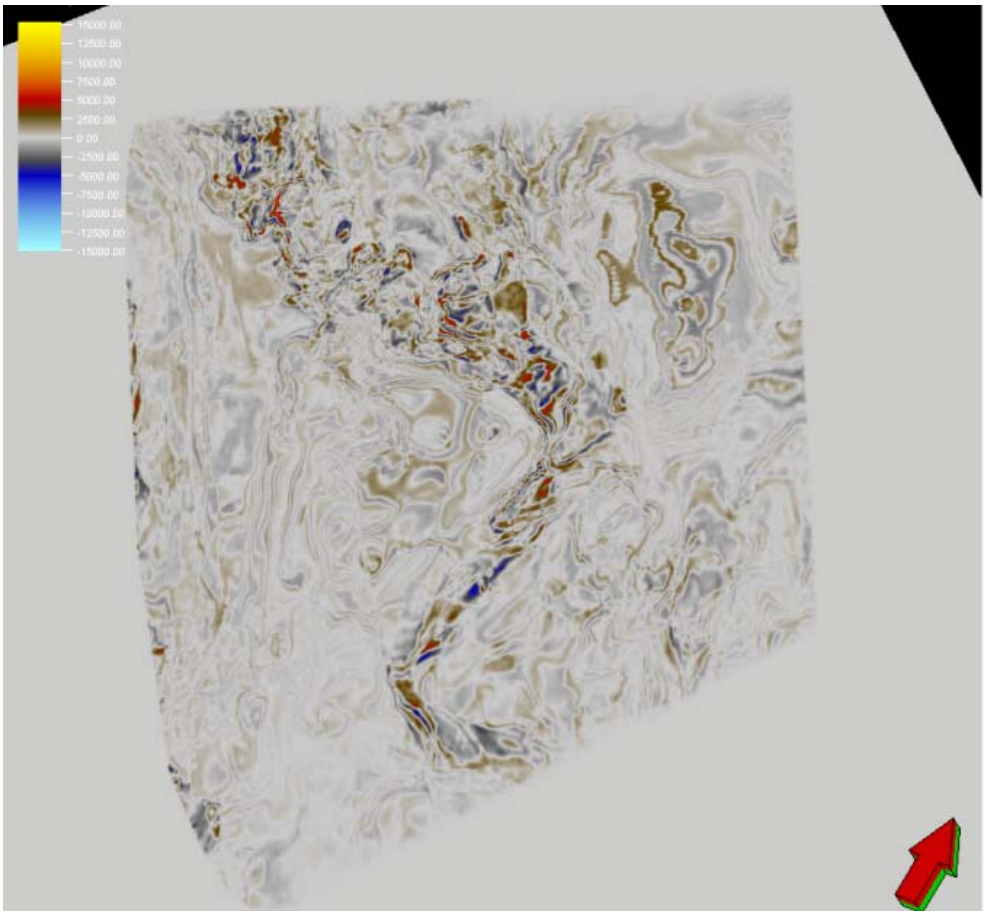

Fig. 11 (a) Relative Acoustic impedance

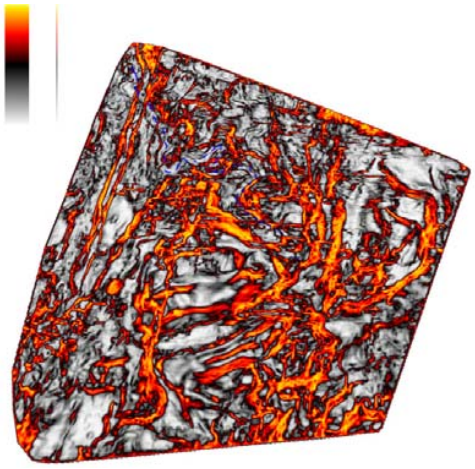

Fig. 11 (b) Variance volume attribute volume attribute

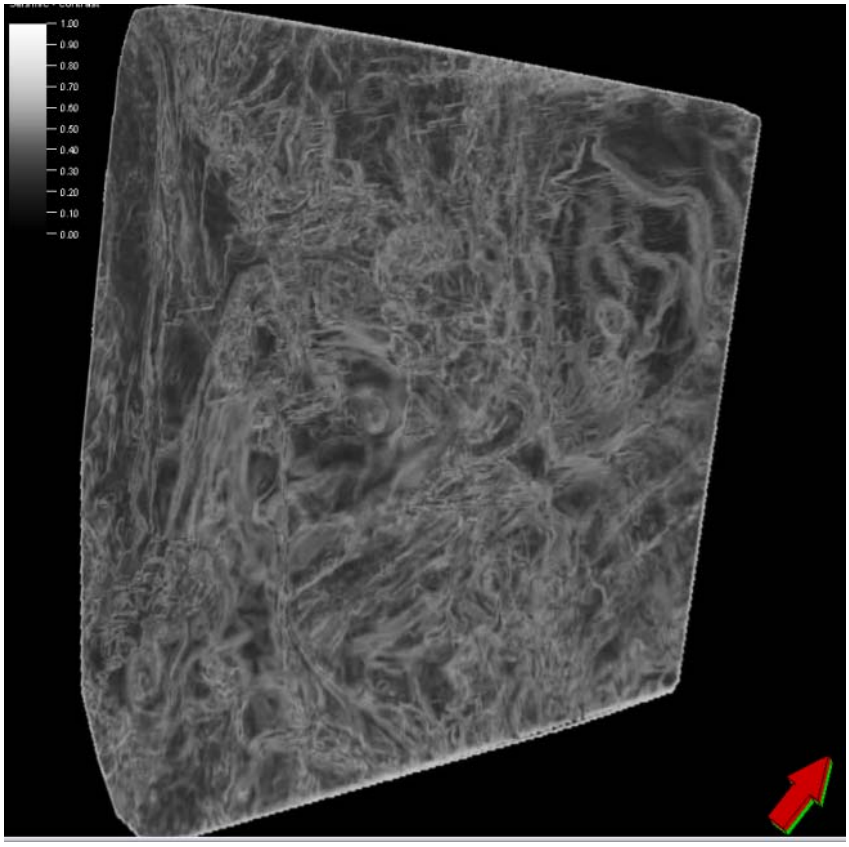

Fig. 11 (c) Amplitude contrast volume attribute

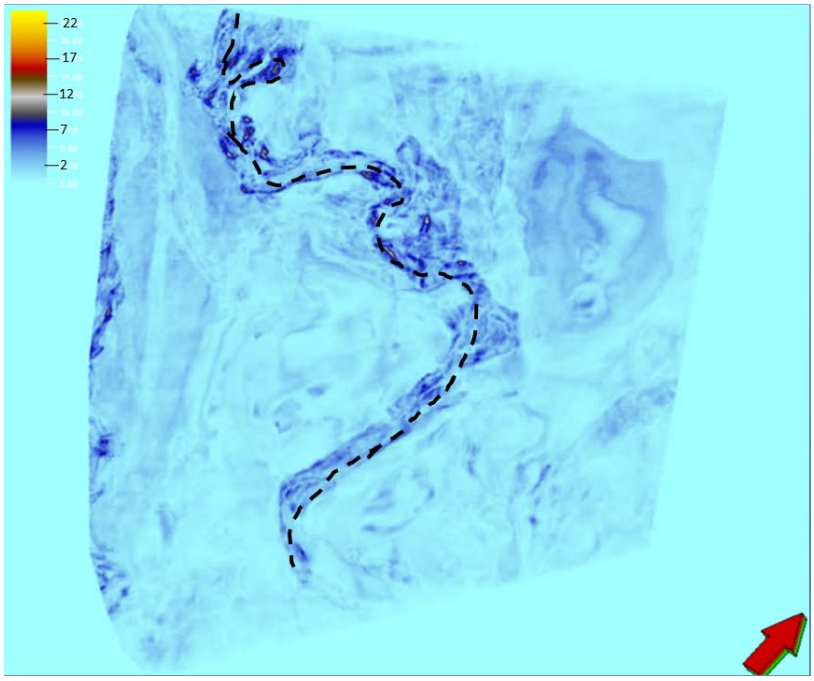

Fig. 11 (d) Reflection intensity volume attribute

- Mass movements in the area are commonly debris flow and mudflow complemented by bedforms at the later stage.
- In this study, Petrel perturbation impulse response was

used to indicate reactions of the dynamic sedimentary geologic processes relating to changes in the nature of sediments transport in a canyon, such as bringing to the surface paleo sediment response to external changes, indicating that the morphology of the canyon also contributed to the sediment transfer direction from NE to NW.

– More study is encouraged to identify the facies in the channel lobe transition and cyclic steps and the role of supercritical flow and hydraulic jumps in lower slopes on the basin floor and the evolution of deep-water depositional systems.

REFERENCES

[1] Shepard, F P, and R F Dill. 1969. "Physiography and Sedimentary Processes of La Jolla Submarine Fan and Fan-Valley , California â€™ La Jolla Submarine Fan and Fan-Valley , California Inadequacy of Piston and Gravity Coring in Penetrating Compacted Sands . After the Initiation of Box Coring (." *Ttie American Association of Petroleum Geologists Bulletin* 2 (2).

[2] Normark, William R, and Paul R Carlson. 2003. "Giant Submarine Canyons: Is Size Any Clue to Their Importance in the Rock Record?" *Geological Society of America, Special Paper 370*, 1–15. doi:10.1130/0-8137-2370-1.175.

[3] Normark, William R, David J W Piper, Brian W Romans, and Jacob A Covault. 2009. "Submarine Canyon and Fan Systems of." *Earth Science in the Urban Ocean: The Southern California Continental Borderland: Geological Society of America Special Paper 454* 2454: 141–68. doi:10.1130/2009.2454(2.7).

[4] Piper, D. J.W., and W. R. Normark. 2009. "Processes That Initiate Turbidity Currents and Their Influence on Turbidites: A Marine Geology Perspective." *Journal of Sedimentary Research* 79 (6): 347–62. doi:10.2110/jsr.2009.046.

[5] Davies, Richard J., Kate E. Thatcher, Simon A. Mathias, and Jinxiu Yang. 2012. "Deepwater Canyons: An Escape Route for Methane Sealed by Methane Hydrate." *Elsevier Earth and Planetary Science Letters* 323–324. Elsevier B.V.: 72–78. doi:10.1016/j.epsl.2011.11.007.

[6] Harris, Peter T, and Tanya Whiteway. 2011. "Global Distribution of Large Submarine Canyons : Geomorphic Differences between Active and Passive Continental Margins." *Marine Geology* 285 (1–4). Elsevier B.V.: 69–86. doi:10.1016/j.margeo.2011.05.008.

[7] Huang, Zhi, Scott L Nichol, Peter T Harris, and M Julian Caley. 2014. "Classi Fi Cation of Submarine Canyons of the Australian Continental Margin." *Marine Geology* 357. Elsevier B.V.: 362–83. doi:10.1016/j.margeo.2014.07.007.

[8] Goldfinger, C., Morey, A.E., Nelson, C.H., Gutie´ Rrez-Pastor, J., Johnson, J.E., Karabanov, E., Chaytor, J., Eriksson, A., And The Shipboard Scientific Party, 2007, Rupture lengths and temporal history of significant earthquakes on the offshore and north coast segments of the Northern San Andreas Fault based on turbidite stratigraphy: Earth and Planetary Science Letters, v. 254, p. 9–27

[9] McGregor, B.A., Stubblefield, W.L., Ryan, W.B.F., Twichell, D.C., 1982. Wilmington submarine canyon: a marine fluvial-like system. Geology 10, 27–30.

[10] Pratson, L.F., Ryan,W.B.F., 1996. Automated drainage extraction in mapping theMonterey Submarine Drainage System, California margin. Marine Geophysical Researches 18, 757–777.

[11] Micallef, A., Mountjoy, J.J., 2011. A topographic signature of a hydrodynamic origin for submarine gullies. Geology 39, 115–118.

[12] Field, M.E., Gardner, J.V., Prior, D.B., 1999. Geometry and significance of stacked gullies on the northern California slope. Marine Geology 154 (1), 271e286.

[13] Izumi, N., 2004, The formation of submarine gullies by turbidity currents: Journal of Geophysical Research, v. 109, doi: 10.1029/2003JC001898.

[14] Chiocci, F.L., Casalbore, D., 2011. Submarine gullies on Italian upper slopes and their rela- tionship with volcanic activity revisited 20 years after Bill Normark's pioneering work. Geosphere 7:1–11. http://dx.doi.org/10.1130/GES00633.

[15] Mountjoy, J.J., Barnes, P.M., Pettinga, J.R., 2009. Morphostructure and evolution ofsubma- rine canyons across an active margin: Cook Strait sector of the Hikurangi Margin, New Zealand. Marine Geology 260, 45–68.

[16] Puga-Bernabeu, A.,Webster, J.M., Beaman, R.J., Guilbaud, V., 2011. Morphology and controls on the evolution of a mixed carbonate-siliciclastic submarine canyon system, Great Barrier Reef margin, north-eastern Australia. Marine Geology 289, 100–116.

[17] Almeida, Narelle Maia de, Helenice Vital, and Moab Praxedes Gomes. 2015. "Morphology of Submarine Canyons along the Continental Margin of the Potiguar Basin, NE Brazil." *Marine and Petroleum Geology* 68. Elsevier Ltd: 307–24. doi:10.1016/j.marpetgeo.2015.08.035.

[18] Puig, Pere, Ruth Durán, Araceli Muñoz, Elena Elvira, and Jorge Guillén. 2017. "Submarine Canyon-Head Morphologies and Inferred Sediment Transport Processes in the Alías-Almanzora Canyon System (SW Mediterranean): On the Role of the Sediment Supply." *Marine Geology* 393. Elsevier B.V.: 21–34. doi:10.1016/j.margeo.2017.02.009.

[19] Pratson, L.F., Nittrouer, C.A., Wiberg, P.L., Steckler, M.S., Cacchione, D.A., Fulthorpe, C.S., Driscoll, N.W., Paola, C., Fedeles, J.J., 2007. Seascape evolution on clastic continental shelves and slopes. In: Nitrouer, C.A., Austin, J.A., Field, M.E., Kravitz, J.H., Syvitski, J.P.M., Wiberg, P.L. (Eds.), Continental-Margin Sedimen- tation: from Sediment Transport to Sequence Stratigraphy, IAP Special Publi- cation 37. Blackwell Publishing, Oxford, pp. 339e380.

[20] Skene, K.I.,Piper, D.J.W., 2006. Late Cenozoic evolution ofLaurentian Fan: development of a glacially-fed submarine fan. Marine Geology 227, 67–92.

[21] Bourget, J., Zaragosi, S., Garlan, T., Gabelotaud, I., Guyomard, P., Dennielou, B., Ellouz- Zimmermann, N., Schneider, J.L., 2008. Discovery of a giant deep-sea valley in the Indian Ocean, off eastern Africa: the Tanzania channel. Marine Geology 255 (3–4), 179–185.

[22] Normark, W. R., J. G. Moore, and M. E. Torresan, Giant volcano-related landslides and the development of the Hawaiian Islands, in Submarine Landslides: Selected Studies in the U.S. Exclusive Economic Zone, edited by W. C. Schwab H. J. Lee, and D.C. Twichell, U.S. Geol. Surv. Bull., 2002, 184-196, 1993.

[23] Covault, Jacob A., Svetlana Kostic, Charles K. Paull, Zoltán Sylvester, and Andrea Fildani. 2017. "Cyclic Steps and Related Supercritical Bedforms: Building Blocks of Deep-Water Depositional Systems, Western North America." *Marine Geology* 393. Elsevier B.V.: 4–20. doi:10.1016/j.margeo.2016.12.009.

[24] Casalbore, Daniele, Domenico Ridente, Alessandro Bosman, and Francesco L. Chiocci. 2017. "Depositional and Erosional Bedforms in Late Pleistocene-Holocene pro-Delta Deposits of the Gulf of Patti (Southern Tyrrhenian Margin, Italy)." *Marine Geology* 385. Elsevier B.V.: 216–27. doi:10.1016/j.margeo.2017.01.007.

[25] Wynn, Russell B., Neil H. Kenyon, Douglas G. Masson, Dorrik A.V. Stow, and Philip P.E. Weaver. 2002. "Characterization and Recognition of Deep-Water Channel-Lobe Transition Zones." *AAPG Bulletin* 86 (8): 1441–62. doi:10.1306/61eedcc4-173e-11d7-8645000102c1865d.

[26] Gong, Chenglin, Yingmin Wang, Xuechao Peng, Weiguo Li, Yan Qiu, and Shang Xu. 2012. "Sediment Waves on the South China Sea Slope off Southwestern Taiwan: Implications for the Intrusion of the Northern Pacific Deep Water into the South China Sea." *Marine and Petroleum Geology* 32 (1). Elsevier Ltd: 95–109. doi:10.1016/j.marpetgeo.2011.12.005.

[27] Dyer, K. R., & Huntley, D. A. (1999). The origin, classification and modelling of sand banks and ridges. Continental ShelfResearch, 19 (10), 1285-1330

[28] Belderson, R. H. (1986). Offshore tidal and non-tidal sand ridges and sheets: differences in morphology and hydrodynamic setting. In R. J. Knight & J. R. McLean (Eds.), Shelf Sands and Sandstones (pp. 293-301). Can. Soc. Petr. Geol.

[29] Guillén, Jorge. 2017. *Atlas of Bedforms in the Western Mediterranean*. doi:10.1007/978-3-319-33940-5.

[30] van Dijk TA, Kleinhans MG (2005) Processes controlling the dynamics of compound sand waves in the North Sea, Netherlands. J Geophys Res Earth 110(F4).

[31] Fildani, A., Normark, W.R., Kostic, S. and Parker, G. (2006) Channel formation by flow stripping: large-scale scour features along the Monterey East Channel and their relation to sediment waves. Sedimentology, 53, 1265–1287.

[32] Kostic, S. 2011. "Modeling of Submarine Cyclic Steps: Controls on Their Formation, Migration, and Architecture." *Geosphere* 7 (2): 294–304. doi:10.1130/GES00601.1.

[33] Cartigny, Matthieu J.B., George Postma, Jan H. van den Berg, and Dick R. Mastbergen. 2011. "A Comparative Study of Sediment Waves and Cyclic Steps Based on Geometries, Internal Structures and Numerical Modeling." *Marine Geology* 280 (1–4). Elsevier B.V.: 40–56. doi:10.1016/j.margeo.2010.11.006.

[34] Hamilton PB, Strom KB, Hoyal DCJD (2015) Hydraulic and sediment transport properties of autogenic avulsion cycles on submarine fans with supercritical distributaries. J Geophys Res doi:10.1002/2014JF003414, in press

[35] Wynn, R B, P P E Weaver, G Ercilla, D a V Stow, and D G Masson. 2000. "Sedimentary Processes in the Selvage Sediment-Wave ¢eld." *NE Atlantic* 47: 1181^1197.

[36] Migeon, S., B. Savoye, E. Zanella, T. Mulder, J. C. Faugères, and O. Weber. 2001. "Detailed Seismic-Reflection and Sedimentary Study of Turbidite Sediment Waves on the Var Sedimentary Ridge (SE France): Significance for Sediment Transport and Deposition and for the Mechanisms of Sediment-Wave Construction." *Marine and Petroleum Geology* 18 (2): 179–208. doi:10.1016/S0264-8172(00)00060-X.

[37] Normark, William R., David J.W. Piper, Henry Posamentier, Carlos Pirmez, and Sébastien Migeon. 2002. *Variability in Form and Growth of Sediment Waves on Turbidite Channel Levees. Marine Geology*. Vol. 192. doi:10.1016/S0025-3227(02)00548-0.

[38] Wynn, Russell B., David J.W. Piper, and Martin J.R. Gee. 2002. "Generation and Migration of Coarse-Grained Sediment Waves in Turbidity Current Channels and Channel-Lobe Transition Zones." *Marine Geology* 192 (1–3): 59–78. doi:10.1016/S0025-3227(02)00549-2.

[39] Ediger, V., A. F. Velegrakis, and G. Evans. 2002. "Upper Slope Sediment Waves in the Cilician Basin, Northeastern Mediterranean." *Marine Geology* 192 (1–3): 321–33. doi:10.1016/S0025-3227(02)00562-5.

[40] Ã, Roger D Flood, and Liviu Giosan. 2002. "12p_Reiner Anderl.pdf" 192: 259–73.

[41] HILL, P.R., 2012, Changes in submarine channel morphology and slope sedimentation patterns from repeat multibeam surveys in the Fraser River delta, western Canada, in Li, M.Z., Sherwood, C.R., and Hill, P.R., eds., Sediments, Morphology and Sedimentary Processes on Continental Shelves: Advances in Technologies, Research and Applications: International Association of Sedimentologists, Special Publication 44, p. 47–70

[42] Arzola, R.G., Wynn, R.B., Lastras, G., Masson, D.G., and Weaver, P.P.E., 2008, Sedimentary features and pro- cesses in the Nazare and Setubal submarine canyons, west Iberian margin: Marine Geology, v. 250, p. 64-88.

[43] Wright, I.C., Worthington, T.J., Gamble, J.A., 2006. New multibeam mapping and geochemistry of the 30–35 S sector, and overview, of southern Kermadec arc volcanism. J. Volcanol. Geotherm. Res. 149, 263–296.

[44] Cattaneo, A., Correggiari, A., Marsset, T., Thomas, Y., Marsset, B., Trincardi, F. (2004). Seafloor undulation pattern on the Adriatic shelf and comparison to deep-water sediment waves. Mar. Geol. 213, 121–148. doi:10.1016/j.margeo.2004.10.004

[45] Symons, William O., Esther J. Sumner, Peter J. Talling, Matthieu J.B. Cartigny, and Michael A. Clare. 2016. "Large-Scale Sediment Waves and Scours on the Modern Seafloor and Their Implications for the Prevalence of Supercritical Flows." *Marine Geology* 371. Elsevier B.V.: 130–48. doi:10.1016/j.margeo.2015.11.009.

[46] Piper, D.J.W., Normark, W.D., 1983. Turbidite depositional patterns and flow characteristics, Navy submarine fan, California borderland. Sedimentology 30, 681–694.

[47] Mutti E, Normark WR (1987) Comparing examples of modern and ancient turbidite systems: problems and concepts. In: Leggett JK, Zuffa GG (eds) Marine clastic sedimentology: concepts and case studies. Graham and Trotman, London, pp 1–38

[48] Cartigny, M.J.B., Postma, G., van den Berg, J.H., Mastbergen, D.R., 2011. A comparative study of sediment waves and cyclic steps based on geometries, internal structures and numerical modeling. Mar. Geol. 280, 40–56. Kostic

[49] Zhong, Guangfa, Matthieu J.B. Cartigny, Zenggui Kuang, and Liaoliang Wang. 2015. "Cyclic Steps along the South Taiwan Shoal and West Penghu Submarine Canyons on the Northeastern Continental Slope of the South China Sea." *Bulletin of the Geological Society of America* 127 (5–6): 804–24. doi:10.1130/B31003.1.

[50] Winterwerp, J.C., Bakker, W.T., Mastbergen, D.R., Van Rossum, H., 1992. Hyperconcen- trated sand–water mixture flows over erodible bed. Journal of Hydraulic Engineering 118 (11), 1508–1525.

[51] Taki, K., and Parker, G., 2005, Transportational cyclic steps created by fl ow over an erodible bed, Part 1, Theory and numerical simulation: Journal of Hydraulic Research, v. 43, p. 488–501, doi: 10.1080/00221680509500147.

[52] Van Den Berg, J.H., Vangelder,A., And Mastbergen, D.R., 2002, The importance of breaching as a mechanism of subaqueous slope failure in fine sand: Sedimentology, v. 49, p. 81–95.

[53] Talling, P. J., J. Allin, D. A. Armitage, R. W. C. Arnott, M. J. B. Cartigny, M. A. Clare, F. Felletti, et al. 2015. "Key Future Directions For Research On Turbidity Currents and Their Deposits." *Journal of Sedimentary Research* 85 (2): 153–69. doi:10.2110/jsr.2015.03.

[54] Yokokawa, M., Okuno, K., Nakamura, A., Muto, T., Miyata, Y., Naruse, H., 2009. Aggradational cyclic steps: sedimentary structures found in flume experiments. Proceedings 33rd IAHR Congress Vancouver.

[55] Fagherazzi, S., and Sun, T., 2003, Numerical simulations of transportational cyclic steps. Computers & Geosci- ences, v. 29, p. 1143–1154, doi: 10 .1016 /S0098 -3004 (03)00133 -X .par

[56] Sun,T., and Parker, G., 2005, Transportational cyclic steps created by flow over an erodible bed. Part 2. Theory and numerical simulation: Journal of Hydraulic Research, v. 43, p. 502–514

[57] Normark, W.R., Piper, D.J.W., Posamentier, H., Pirmez, C., Migeon, S., 2002. Variability in form and growth of sediment waves on turbidite channel levees. Mar. Geol. 192, 23–58.

[58] Ercilla, Gemma, Belén Alonso, Russell B. Wynn, and Jesús Baraza. 2002. "Turbidity Current Sediment Waves on Irregular Slopes: Observations from the Orinoco Sediment-Wave Field." *Marine Geology* 192 (1–3): 171–87. doi:10.1016/S0025-3227(02)00554-6.

[59] Lastras, G., Acosta, J., Mu~noz, A., Canals, M., 2011. Submarine canyon formation and evolution in the Argentine Continental Margin between 44?30'S and 48?S. Geomorphology 128 (3e4), 116e136

[60] Lo Iacono, C., Sulli, A., Agate, M., 2014. Submarine canyons of north-western Sicily (Southern Tyrrhenian Sea): variability in morphology, sedimentary processes and evolution on a tectonically active margin. Deep Sea Res. II 104, 93e105.

[61] Micallef, A., Mountjoy, J.J., Barnes, P.M., Canals, M., Lastras, G., 2014. Geomorphic response of submarine canyons to tectonic activity: insights from the Cook Strait canyon sys- tem, New Zealand. Geosphere 10, 905–929.

[62] Bastos, Ildeson Prates. 2000. "Ceara Basin," no. Gouyet 1988: 2000.

[63] Jovane, Luigi, Jorge J. P. Figueiredo, Daniel P. V. Alves, David Iacopini, Martino Giorgioni, Paola Vannucchi, Denise S. Moura, et al. 2016. "Seismostratigraphy of the Ceará Plateau: Clues to Decipher the Cenozoic Evolution of Brazilian Equatorial Margin." *Frontiers in Earth Science* 4 (October): 1–14. doi:10.3389/feart.2016.00090.

[64] Golonka, Jan, Robert Pauken Ñ Mobil, and New Exploration. 2015. "Phanerozoic Paleoenvironment and Lithofacies Maps of the Circum-Atlantic Margins," no. January 1998: 432–33.

[65] CLARK, Ian R., and JOSEPH A. Cartwright. 2012. "Interactions between Coeval Sedimentation and Deformation from the Niger Delta Deepwater Fold Belt." *SEPM Special Publication*, no. 99: 243–67. doi:10.2110/pec.12.99.0243.

[66] Burke, K, TFJ Dessauvagie, and AJ Whiteman. 1971. "Opening of the Gulf of Guinea and Geological History of the Benue Depression and Niger Delta." *Nature* 233: 51–55. doi:doi:10.1038/physci233051a0.

[67] Fairhead, J. D., and R. M. Binks. 1991. "Differential Opening of the Central and South Atlantic Oceans and the Opening of the West African Rift System." *Tectonophysics* 187 (1–3): 191–203. doi:10.1016/0040-1951(91)90419-S.

[68] Jolly, Byami A., Lidia Lonergan, and Alexander C. Whittaker. 2016. "Growth History of Fault-Related Folds and Interaction with Seabed Channels in the Toe-Thrust Region of the Deep-Water Niger Delta." *Marine and Petroleum Geology* 70. Elsevier Ltd: 58–76. doi:10.1016/j.marpetgeo.2015.11.003.

[69] Maestrelli, D, D Iacopini, V Maselli, N Scarselli, P Vannucchi, L Jovane, and B Kneller. 2018. "Submarine Depression Trails Driven by the Interplay of Density Currents and Fluid Migration .," no. July.

[70] Matos, R.M.D., 1999. History of the northeast Brazilian rift system: kinematics im- plications for the break-up between Brazil and West Africa. In: Cameron, N.R., Bate, R.H., Clure, V.S. (Eds.), The Oil and Gas Habitats of the South Atlantic, Geological Society, London, Special Publications, 155, pp. 55e73.

[71] Bertani, R.T., Costa, L.G., Matos, R.M.D., 1990. Tectonic-sedimentary evolution, structural style and oil habitat in the Potiguar Basin. In: Raja Gabaglia, G.P., Milani, E.J. (Eds.), Origin and Evolution of Sedimentary

Basins. Petrobras, Rio de Janeiro, pp. 291e310 (in Portuguese)
[72] Maselli, B. Kneller, O.L. Taiwo, D. Iacopinib V. 2019. "Sea Floor Bedforms and Their Influence on Slope Accommodation." *Marine and Petroleum Geology 102 (2019) 625–637 Contents* 102: 625–37. doi:10.31223/osf.io/ph6fm.
[73] Normandeau, Alexandre, Patrick Lajeunesse, Antoine G. Poiré, and Pierre Francus. 2016. "Morphological Expression of Bedforms Formed by Supercritical Sediment Density Flows on Four Fjord-Lake Deltas of the South-Eastern Canadian Shield (Eastern Canada)." *Sedimentology* 63 (7): 2106–29. doi:10.1111/sed.12298.
[74] Masson, DG, TP Le Bas, B J Bett, V Huhnerbach, CL Jacobs, and R B Wynn. 2003. "Seafloor Sediments and Sedimentary Processes on the Outer Continental Shelf, Continental Slope and Basin Floor." *Strategic Environmental Assessment: SEA 4. Consultation Document*, no. 4: 51pp.
[75] Guillén, Jorge. 2017. *Atlas of Bedforms in the Western Mediterranean*. doi:10.1007/978-3-319-33940-5.
[76] Tubau, Xavier, Charles K Paull, Galderic Lastras, David W Caress, Miquel Canals, Eve Lundsten, Krystle Anderson, Roberto Gwiazda, and David Amblas. 2015. "Submarine Canyons of Santa Monica Bay , Southern California : Variability in Morphology and Sedimentary Processes." *Marine Geology* 365. Elsevier B.V.: 61–79. doi:10.1016/j.margeo.2015.04.004.
[77] Kneller, Ben, Mason Dykstra, Luke Fairweather, and Juan Pablo Milana. 2016. "Mass-Transport and Slope Accommodation: Implications for Turbidite Sandstone Reservoirs." *AAPG Bulletin* 100 (2): 213–35. doi:10.1306/09011514210.
[78] Jobe, Zane R, Donald R Lowe, and Steven J Uchytil. 2011. "Two Fundamentally Different Types of Submarine Canyons along the Continental Margin of Equatorial Guinea." *Marine and Petroleum Geology* 28 (3). Elsevier Ltd: 843–60.
[79] Maier, Katherine L., Daniel S. Brothers, Charles K. Paull, Mary McGann, David W. Caress, and James E. Conrad. 2017. "Records of Continental Slope Sediment Flow Morphodynamic Responses to Gradient and Active Faulting from Integrated AUV and ROV Data, Offshore Palos Verdes, Southern California Borderland." *Marine Geology* 393. Elsevier B.V.: 47–66.
[80] Posamentier, Henry W., and Venkatarathnan Kolla. 2003. "Seismic Geomorphology and Stratigraphy of Depositional Elements in Deep-Water Settings." *Journal of Sedimentary Research* 73 (3): 367–88. doi:10.1306/111302730367.
[81] Paull, C. K., W. Ussler III, D. W. Caress, E. Lundsten, J. A. Covault, K. L. Maier, J. Xu, and S. Augenstein. 2010. "Origins of Large Crescent-Shaped Bedforms within the Axial Channel of Monterey Canyon, Offshore California." *Geosphere* 6 (6): 755–74. doi:10.1130/GES00527.1.
[82] Smith, D.P., Kvitek, R., Iampietro, P.J., Wong, K., 2007. Twenty-ninemonths ofgeomorphic change in upper Monterey Canyon (2002–2005). Mar. Geol. 236, 79–94.
[83] Postma, George, Kick Kleverlaan, and Matthieu J.B. Cartigny. 2014. "Recognition of Cyclic Steps in Sandy and Gravelly Turbidite Sequences, and Consequences for the Bouma Facies Model." *Sedimentology* 61 (7): 2268–90. doi:10.1111/sed.12135.
[84] Sequeiros, Octavio E. 2012. "Estimating Turbidity Current Conditions from Channel Morphology: A Froude Number Approach." *Psychological Reports* 117 (3 Pt 2): 819–22. doi:10.1029/2011JC007201.
[85] Postma, G., Cartigny, M.J.B., Kleverlaan, K., 2009. Structureless, coarse-tail graded bouma Ta formed by internal hydraulic jump of the turbidity current? Sediment. Geol. 219, 1–6.
[86] Covault, Jacob A., Svetlana Kostic, Charles K. Paull, Holly F. Ryan, and Andrea Fildani. 2014. "Submarine Channel Initiation, Filling and Maintenance from Sea-Floor Geomorphology and Morphodynamic Modelling of Cyclic Steps." *Sedimentology* 61 (4): 1031–54. doi:10.1111/sed.12084.
[87] Einsele, Gerhard. 1992. *Gerhard Einsele. Springer-Verlag Berlin Heidelberg New York London Paris Tokyo Hong Kong Barcelona Budapest*. Springer-Verlag Berlin Heidelberg New York London Paris Tokyo Hong Kong Barcelona Budapest. doi:Springer-Verlag Berlin Heidelberg New York London Paris Tokyo Hong Kong Barcelona Budapest.
[88] Xu, J.P., Wong, F.L., Kvitek, R., Smith, D.P. and Paull, C.K. (2008) Sandwave migration in Monterey Submarine Canyon, Central California. Mar. Geol., 248, 193–212.
[89] Rahman, Syed Mustafizur, M Rezaul Islam, and Mumnunul Keramat. 2008. "Seismic Imaging by Impulse Response for Studying Crustal Structure of the Central Tibet." *Journal of Scientific Research* 1 (1): 61–71. doi:10.3329/jsr.v1i1.1082.
[90] Frey-Martinez, J. 2010. "3D Seismic Interpretation of Mass Transport Deposits : Implications for Basin Analysis and Geohazard Evaluation." *Advances in Natural and Technological Hazards Research, Vol 28, © Springer Science + Business Media B.V. 2010* 28.
[91] Geoffroy, Lamarche Joanne, Cathy, and Jean-yves Collot. 2008. "Successive, Large Mass-Transport Deposits in the South Kermadec Fore-Arc Basin, New Zealand: The Matakaoa Submarine Instability Complex," no. 4219. doi:10.1029/2007GC001843.
[92] Kastens, K.A., Shor, A.N., 1985. Depositional processes of a meandering channel on Mississippi fan. AAPG Bulletin 69, 190–202.
[93] Schwab, A.M., Tremblay, S. and Hurst, A., 2007. Seismic expression of turbidity-current and bottom-current processes on the Northern Mauritanian continental slope. In: R.J. Davies, H. Posamentier, L. Wood and J. Cartwright (Eds.), Seismic Geomorphology. Geological Society of London, Special Publications, 277, pp. 237-252.